

Waves in Random and Complex Media

ISSN: (Print) (Online) Journal homepage: <https://www.tandfonline.com/loi/twrm20>

Thermosolutal Marangoni convection on a permeable flat surface with aligned magnetic field and thermophoretic effect: an OHAM solution

Anil Kumar Gautam, Amit Kumar Pandey, Krishnendu Bhattacharyya, Kottakkaran Sooppy Nisar, Ali J. Chamkha & Dhananjay Yadav

To cite this article: Anil Kumar Gautam, Amit Kumar Pandey, Krishnendu Bhattacharyya, Kottakkaran Sooppy Nisar, Ali J. Chamkha & Dhananjay Yadav (2023): Thermosolutal Marangoni convection on a permeable flat surface with aligned magnetic field and thermophoretic effect: an OHAM solution, Waves in Random and Complex Media, DOI: [10.1080/17455030.2023.2171152](https://doi.org/10.1080/17455030.2023.2171152)

To link to this article: <https://doi.org/10.1080/17455030.2023.2171152>



Published online: 09 Mar 2023.



Submit your article to this journal [↗](#)



Article views: 62



View related articles [↗](#)



View Crossmark data [↗](#)



Thermosolutal Marangoni convection on a permeable flat surface with aligned magnetic field and thermophoretic effect: an OHAM solution

Anil Kumar Gautam^a, Amit Kumar Pandey^a, Krishnendu Bhattacharyya^a,
Kottakkaran Sooppy Nisar^b, Ali J. Chamkha^c and Dhananjay Yadav^d

^aDepartment of Mathematics, Institute of Science, Banaras Hindu University, Varanasi, India; ^bDepartment of Mathematics, College of Arts and Sciences, Prince Sattam bin Abdulaziz University, Wadi Aldawaser, Saudi Arabia; ^cFaculty of Engineering, Kuwait College of Science and Technology, Doha District, Kuwait; ^dDepartment of Mathematical and Physical Sciences, University of Nizwa, Birkat Al Mawz, Oman

ABSTRACT

In this venture, the challenge to study the mathematical model and its approximate solution for boundary layer thermosolutal Marangoni convection on a permeable flat surface with thermophoretic velocity and aligned magnetic field has been undertaken. Using a special type of transformation, governing PDEs are converted into ODEs. A semi-analytical method known as optimal homotopy analysis method (OHAM) has been used to develop solutions for proposed mathematical model. The novelty of the study is in the exploration of simultaneous impacts of thermophoretic velocity and inclined magnetic field on flow and heat-mass transport while mass suction/injection is using OHAM. Solutions obtained by OHAM are compared with other published literature and it is revealed that our numerical values are improved by approximately up to 7%. The obtained solutions for various important parameters are displayed in the form of graphs and tables. The study explores the variable behaviors of velocity, temperature, and concentration for growths of Marangoni number, magnetic parameter, and thermophoretic parameter, while there exists mass suction or injection. It reveals that in both cases, i.e. suction and injection cases, velocity grows and temperature and concentration reduce with increasing magnetic parameters and inclination angle of aligned magnetic field and these variations are more prominent in case injection. If the magnetic field is orthogonal to the flat surface, then corresponding Lorentz force produces maximum resistance for the transport phenomenon. The spreading effect of induced surface velocity due to Marangoni convection is observed in the entire boundary layer region in case of mass suction, while for injection case it is witnessed only near the surface. Whereas, for higher value of thermophoretic velocity, the concentration exhibits a reducing trend. For rising

ARTICLE HISTORY

Received 27 December 2021
Accepted 31 October 2022

KEYWORDS

Thermosolutal Marangoni convection; aligned magnetic field; permeable flat surface; thermophoretic velocity; OHAM solution

values of Marangoni number, wall velocity, Nusselt number, and Sherwood number significantly grow, while magnetic field has contrary impacts.

Nomenclature

A, A^*	Positive constants
B_0	Applied magnetic field
C	Volumetric concentration of the fluid
C_1, C_2	Coefficient involve in special transformation
C_w	Variable wall concentration
C_∞	Fixed concentration away from the plate
D_B	Mass diffusivity
f	Dimensionless velocity
k	Thermophoretic coefficient
L	Characteristic length
M	Magnetic parameter
Ma	Thermosolutal surface tension ratio (Marangoni number)
Nu_x	Local Nusselt number
Pr	Prandtl number
ρ_w	Mass flux
q_w	Heat flux at the wall
Sc	Schmidt number
Sh_x	Local Sherwood number
T	Temperature of the fluid
T_r	Reference temperature
T_w	Variable wall temperature
T_∞	Fixed temperature away from the plate
(u, v)	Velocity components along x -axis and y -axis respectively
Vc	Suction/injection parameter
V_T	Thermophoretic coefficient
v_w	Suction or injection velocity
(x, y)	Space coordinates

Greek symbols

α^*	Angle with the surface
β	Thermal diffusivity
γ_T	Temperature coefficient
γ_C	Concentration coefficient
$\Delta T, \Delta C$	Characteristic temperature and concentration, respectively
ν	Kinematic viscosity
μ	Dynamic viscosity
δ_0	Electrical conductivity

ρ	Density
σ	Surface tension
σ^*	Minimum surface tension
τ	Thermophoretic parameter
κ	Thermal conductivity
ϕ	Volumetric concentration
θ	Temperature distribution
ψ	Stream function
η	Dimensionless variable

1. Introduction

Inquiry of interconnections of heat transfer and mass transfer and their endorsements on flow behavior is crucial and their interconnections need to be explored by conceptual and exploratory investigations due to their extensive applications in geothermal systems, evaporation of liquid in a product system, for storage of energy in different forms, reactors of catalytic type, management of different types of nuclear waste, etc.

In 1904, Prandtl presented an interesting and amazing theory, named boundary layer theory. Using the asset of Prandtl's boundary layer investigation, many other researchers also included some wings on this established theory with various types of physical modeling. Tsou et al. [1] investigated the boundary layer over a moving surface with the transfer of heat. Aydin and Kaya [2] reported the variation analysis of boundary layer over a flat plate that is permeable. In addition, Hussain et al. [3] focused on variable surface temperature, species concentration on the permeability of a flat surface in the appearance of natural convection. Aziz [4] discussed the similarity approach for flat plate flow with convective boundary condition.

The area of mechanics in which the analysis of magnetic field and behavior of electricity-conducting fluid are characterized is identified as magnetohydrodynamics(MHD). The phenomenon, MHD is influential due to its wide implementations in different types of fluid flow problems, as well as, its extraordinary role in engineering contexts. The applications of MHD flow are found in the process of energy conversion, in some biomedical problems, like targeted drug delivery and balancing blood circulation. Glauert [5] contributed a remarkable investigation on a flat plate with the MHD effect. Pop and Na [6] explained the consequences of the permeability parameter over an expanding plate in the context of MHD flow.

The term convection is used for the transfer of some liquid-type material from one front to another front. Marangoni convection is a different kind of convection that is instigated by influences in surface tension across a liquid. In the meaning of boundary layer, the Marangoni layers are the dissipative layers and those may happen across the combination of liquid with liquid or liquid with gas. In a situation, when the heat source and temperature gradient are responsible for the thermal inequality between two or more than two consecutive layers of fluid, then Marangoni thermal effect has occurred, whereas the beginning of the Marangoni solutal effect is seen, when the imbalance of the interfacial region, chemical reaction with concentration gradient are responsible. Marangoni convection plays a key role in the zone of chemical engineering and Levich [7] explained it. Magyari and Chamkha

[8,9] revealed that the important factor for Marangoni convection is surface tension gradient and they described MHD Marangoni effect using an analytical approach. Pascal and D'Alessio [10] investigated stability analysis of thermosolutal effects with binary-type liquid. The reason for continuous interest in the field of thermosolutal effect with Marangoni convection is that it has several types of applications in many engineering as well as non-engineering sectors. Some of them are materials processing, the techniques of growing crystal and the process of coating the materials. The initial establishments in the context of Marangoni boundary layers were fixed by Napolitano and Golia [11] and the mixed convection analysis was stated by Chamkha et al. [12]. Tadmor [13] reported a survey on the Marangoni effect. In the last few years, scientists and researchers gave much attention to MHD flow and thermosolutal effect on it. Zhang and Zheng [14] investigated MHD flow with thermosolutal Marangoni convection with the existence of a chemical reaction. Heat generation/absorption in MHD Marangoni convection was clarified by Al-Mudhaf and Chamka [15]. Mahdy and Ahmed [16] looked at the consequences of Soret and Dufour on MHD flow with Marangoni consideration. The thermosolutal Marangoni convection with chemical reaction in porous media was exposed by Mahabaleshwar et al. [17]. Al-Mdallal et al. [18] and Hakeem et al. [19] considered Marangoni convection of various hybrid nanofluids on a permeable flat plate with the existence of an aligned magnetic field and thermal radiation. Nanofluids have a remarkable impact on the heat transfer character of flow dynamics. So, mathematical and numerical modeling of convection flows with nanofluids under consideration accompanied by Marangoni convection is impactful because of engineering and industrial usages. Several important studies on nanofluids and its influence on several flow characteristics are available in the literature [20–35] having excellent findings.

Thermophoresis is a phenomenon in which temperature gradient causes the enhancement of movement of small particles in the hot region and dispersion of those to the cold region, and the velocity induced in this process is recognized as thermophoretic velocity. The effect of this thermophoretic velocity has a vital role in different engineering sectors, such as in combustion devices. Also, small particles in a moving fluid may be removed by thermophoretic velocity. For industrial purposes, the process of heat transfer consists of both thermophoresis and hydromagnetic flow, e.g. MHD energy systems. Initiative study in the context of thermophoresis of suspended particles in the boundary layer concept was discussed by Talbot et al. [36]. The time-dependent behavior of thermophoretic velocity was investigated by Uddin and Ali [37]. Bakier and Gorla [38] explored the impression of thermophoresis on flow along with a vertical plate. Influences of thermophoresis particle sublimation in porous media were dealt with by Postelnicu [39]. Kundu et al. [40] looked at the consequence of thermophoretic velocity and chemical reaction of mixed convective MHD flow. Parida et al. [41] investigated the impact of thermal radiation and thermophoresis variations on MHD flow with the presence of slip. Selim et al. [42] discussed the consequences of thermophoresis on mixed convective flow on a vertical permeable flat plate. Chamkha and Issa [43] reported the heat and mass transfer analysis with thermophoresis and heat generation/absorption on a flat surface. Alam et al. [44–46] considered the thermophoresis effect over a permeable flat surface with different flow geometry and showed the importance of the permeability of the surface as well as thermophoretic velocity on heat and mass transfer analysis.

Motivated by aforementioned facts on the impacts of Marangoni convection and thermophoresis on MHD flows and due to a keen interest to understand their influence when

the magnetic field is aligned and when the flow happens on a porous flat surface, here we modeled a problem to search simultaneous impacts of suction/injection, Marangoni effect, thermophoretic velocity and aligned magnetic field on MHD flow over a permeable flat surface. To achieve solutions, a strong semi-analytical method, optimal homotopy analysis method (OHAM), is implemented. The novelty of the present investigation is to obtain the outcomes of concurrent impacts of the thermophoretic phenomenon and inclined magnetic field on the flow field and heat-mass transport in presence of suction/injection with the help of a semi-analytical approach. Furthermore, We shall try to address the following interesting research issues:

- How suction/injection will affect the impact of magnetic field and its alignment?
- To know the interaction of Marangoni effect and suction/injection
- To understand the dependency of effect of thermophoresis on suction/injection
- To disclose the simultaneous influences of thermosolutal Marangoni convection and aligned magnetic field on heat and mass transfer in presence of suction/injection.

We strongly feel that the proposed modeled investigation will contribute to the literature with its originality and novelty.

2. Mathematical formulation

Consider boundary layer thermosolutal Marangoni convection over a permeable flat surface in presence of aligned magnetic field and thermophoretic velocity. Two coordinate axes x and y are supposed along and perpendicular to the surface. So, the fundamental governing convection equations are [14,16,18]:

$$\frac{\partial u}{\partial x} + \frac{\partial v}{\partial y} = 0, \quad (1)$$

$$u \frac{\partial u}{\partial x} + v \frac{\partial u}{\partial y} - \nu \frac{\partial^2 u}{\partial y^2} + \frac{\delta_0 B_0^2 u}{\rho} \sin^2 \alpha = 0, \quad (2)$$

$$u \frac{\partial T}{\partial x} + v \frac{\partial T}{\partial y} - \beta \frac{\partial^2 T}{\partial y^2} = 0, \quad (3)$$

$$u \frac{\partial C}{\partial x} + v \frac{\partial C}{\partial y} - D_B \frac{\partial^2 C}{\partial y^2} + \frac{\partial}{\partial y} (V_T (C - C_\infty)) = 0. \quad (4)$$

Here u and v are assumed as velocity components along x - and y -axes, respectively, T and C are temperature and concentration, respectively, ν and δ_0 are kinematic viscosity and electrical conductivity, respectively. We supposed that B_0 is a uniform aligned magnetic field, applied in the direction having angle α with the surface. A physical sketch of the mathematical model is exhibited in Figure 1.

The V_T is thermophoretic velocity. It is explained by Talbot et al. [36] and defined as

$$V_T = -\frac{k\nu}{T_r} \frac{\partial T}{\partial y}. \quad (5)$$

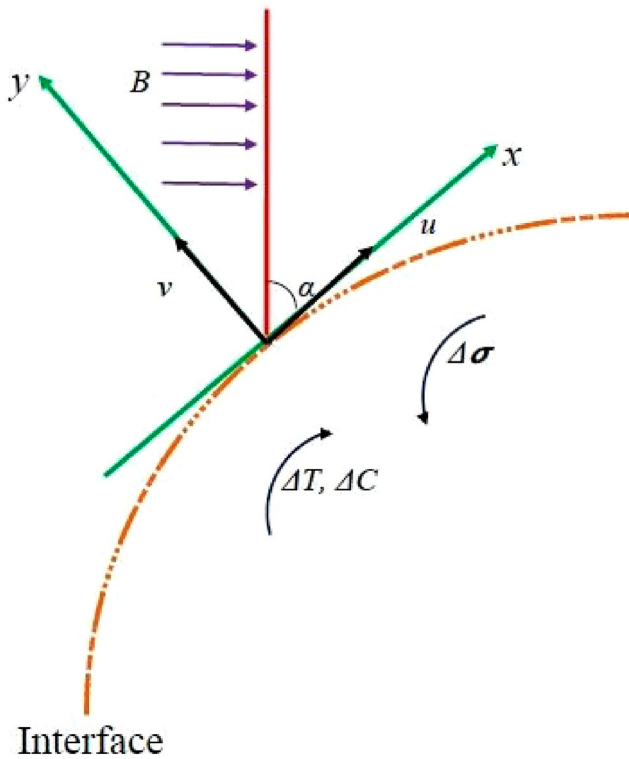


Figure 1. Physical sketch of the mathematical model.

In Equation (5), T_r and k are reference temperature and thermophoretic coefficient, respectively. The thermophoretic parameter is defined as $\tau = -\frac{k(T_w - T_\infty)}{T_r}$.

Now, the dependency of surface tension at the combination of temperature and concentration can be defined by the linear relation as [14]:

$$\sigma = \sigma^* - \gamma_T(T - T_\infty) - \gamma_C(C - C_\infty),$$

where σ^* is the minimum surface tension with $\gamma_T = (\partial\sigma/\partial T)|_C$ and $\gamma_C = (\partial\sigma/\partial C)|_T$ being respectively the temperature coefficient and concentration coefficient of surface tension.

The boundary conditions for constructed physical model are [47,48,14,15]

$$\left. \begin{aligned} \mu \left(\frac{\partial u}{\partial y} \right) &= \gamma_T \left(\frac{\partial T}{\partial x} \right) + \gamma_C \left(\frac{\partial C}{\partial x} \right), \quad v = v_w, \\ T = T_w = T_\infty + Ax^2, \quad C = C_w = C_\infty + A^*x^2 \end{aligned} \right\} \text{at } y \rightarrow 0, \quad (6)$$

$$u = 0, \quad T = T_\infty, \quad C = C_\infty \text{ at } y \rightarrow \infty, \quad (7)$$

where T_w and C_w are variable wall temperature and concentration, respectively, T_∞ and C_∞ are fixed temperature and concentration away from the plate, respectively, $A = \frac{\Delta T}{L^2}$ and $A^* = \frac{\Delta C}{L^2}$ are positive constants with ΔT , ΔC and L being characteristic temperature, concentration and length [49,50], respectively, and mass transfer velocity is v_w ($v_w < 0/v_w > 0$ for suction/injection).

The special type of transformations are defined as [14]

$$\eta = C_1 y, \psi(x, y) = \frac{x f(\eta)}{C_2}, \theta(\eta) = \frac{T - T_\infty}{T_w - T_\infty}, \phi(\eta) = \frac{C - C_\infty}{C_w - C_\infty} \quad (8)$$

where $C_1 = \sqrt[3]{\frac{\rho A \gamma T}{\mu^2}}$ and $C_2 = \sqrt[3]{\frac{\rho^2}{\mu A \gamma T}}$ are constants and ψ is the stream function defined as

$$u = \frac{\partial \psi}{\partial y} \text{ and } v = -\frac{\partial \psi}{\partial x}. \quad (9)$$

Using Equations (8) and (9) in Equations (2)–(4), we get resulting forms of Equations (2)–(4) as

$$f''' - M f' \sin^2 \alpha - f'^2 + f f'' = 0, \quad (10)$$

$$\theta'' - 2 \text{Pr} f' \theta + \text{Pr} \theta' f = 0, \quad (11)$$

$$\phi'' - 2 f' \phi \text{Sc} + f \phi' \text{Sc} - \tau \text{Sc} (\theta' \phi' + \phi \theta'') = 0 \quad (12)$$

with

$$\left. \begin{aligned} f(0) &= Vc, \quad f'(\infty) = 0, \quad f''(0) = -2(1 + Ma), \\ \theta(0) &= 1, \quad \theta(\infty) = 0, \quad \phi(0) = 1, \quad \phi(\infty) = 0. \end{aligned} \right\} \quad (13)$$

The symbols involved in the above equations have the following meanings: $M = \frac{\delta_0 \beta_0^2}{\rho} \sqrt[3]{\frac{\rho \mu}{A^2 [\gamma T]^2}}$ is the magnetic parameter, $\text{Pr} = \frac{\nu}{\beta}$ is the Prandtl number, $\text{Sc} = \frac{\nu}{D_B}$ is the Schmidt number, $Vc = -v_w \sqrt[3]{\frac{\rho^2}{\mu A \gamma T}}$ is the suction/injection parameter, and $Ma = \frac{A^* \gamma C}{A \gamma T}$ is the thermosolutal Marangoni number.

Now, we may develop the surface velocity $u(x, 0)$ as [15]

$$u(x, 0) = \frac{C_1}{C_2} x f'(0). \quad (14)$$

For an engineering point of view, the physical quantities related to heat and mass transfer, local Nusselt number, and local Sherwood number are expressed as

$$\left. \begin{aligned} Nu_x &= \frac{x q_w}{\kappa (T_w - T_\infty)}, \\ Sh_x &= \frac{x p_w}{D_B (C_w - C_\infty)} \end{aligned} \right\} \quad (15)$$

where the heat flux and mass flux at the surface are

$$q_w = -\kappa \left(\frac{\partial T}{\partial y} \right)_{y=0} \text{ and } p_w = -D_B \left(\frac{\partial C}{\partial y} \right)_{y=0}. \quad (16)$$

With the implementation of relations in (8), the resulting forms for the local Nusselt number and local Sherwood number are obtained as [15]

$$Nu_x = -C_1 x \theta'(0) \text{ and } Sh_x = -C_1 x \phi'(0). \quad (17)$$

3. Solution methodology

The optimal homotopy analysis method (OHAM) is one of the few popular semi-analytical methods to get solutions to many mathematical and engineering problems. The whole credit of the establishment and application of the OHAM method to the differential equations goes to Liao [51]. Some of the basic terminologies in this method are

The initial guesses for OHAM solutions as

$$f_0(\eta) = Vc + 2(1 + Ma)(1 - e^{-\eta}), \quad \theta_0(\eta) = e^{-\eta}, \quad \phi_0(\eta) = e^{-\eta} \quad (18)$$

and the defined linear operators as

$$L_f = \frac{d^3}{d\eta^3} - \frac{d}{d\eta}, \quad L_\theta = \frac{d^2}{d\eta^2} - 1, \quad L_\phi = \frac{d^2}{d\eta^2} - 1, \quad (19)$$

with

$$L_f[c_0 + c_1e^\eta + c_2e^{-\eta}] = 0, \quad L_\theta[c_3e^\eta + c_4e^{-\eta}] = 0, \quad L_\phi[c_5e^\eta + c_6e^{-\eta}] = 0, \quad (20)$$

where $c_0, c_1, c_2, c_3, c_4, c_5,$ and c_6 are arbitrary constant.

We choose the auxiliary parameters or convergence control parameters $h_f, h_\theta,$ and h_ϕ and the embedding variable p for exploring zeroth-order and m th-order deformations in the context of the present problem.

3.1. Zeroth-order deformation

$$(1 - p)L_f[\bar{F}(\eta; p) - f_0(\eta)] = ph_fR_fN_f[\bar{F}(\eta; p)] \quad (21)$$

$$(1 - p)L_\theta[\bar{\Theta}(\eta; p) - \theta_0(\eta)] = ph_\theta R_\theta N_\theta[\bar{F}(\eta; p), \bar{\Theta}(\eta; p)], \quad (22)$$

$$(1 - p)L_\phi[\bar{\Phi}(\eta; p) - \phi_0(\eta)] = ph_\phi R_\phi N_\phi[\bar{F}(\eta; p), \bar{\Theta}(\eta; p), \bar{\Phi}(\eta; p)], \quad (23)$$

$$\bar{F}(0; p) = Vc, \quad \bar{F}'(\infty; p) = 0, \quad \bar{F}''(0; p) = -2(1 + Ma), \quad (24)$$

$$\bar{\Theta}(0; p) = 1, \quad \bar{\Theta}(\infty; p) = 0, \quad (25)$$

$$\bar{\Phi}(0; p) = 1, \quad \bar{\Phi}(\infty; p) = 0. \quad (26)$$

The definitions of operators are

$$N_f[F(\eta; p)] = \frac{\partial^3 F(\eta; p)}{\partial \eta^3} + F(\eta; p) \frac{\partial^2 F(\eta; p)}{\partial \eta^2} - M \frac{\partial F(\eta; p)}{\partial \eta} \sin^2 \alpha - \left[\frac{\partial F(\eta; p)}{\partial \eta} \right]^2, \quad (27)$$

$$N_\theta[F(\eta; p), \Theta(\eta; p)] = \frac{\partial^2 \Theta(\eta; p)}{\partial \eta^2} - 2 \text{Pr} \Theta(\eta; p) \frac{\partial F(\eta; p)}{\partial \eta} + \text{Pr} \frac{\partial \Theta(\eta; p)}{\partial \eta} F(\eta; p), \quad (28)$$

$$N_\phi[F(\eta; p), \Theta(\eta; p), \Phi(\eta; p)] = \frac{\partial^2 \Phi(\eta; p)}{\partial \eta^2} - 2Sc \left(\Phi(\eta; p) \frac{\partial F(\eta; p)}{\partial \eta} + \frac{\partial \Phi(\eta; p)}{\partial \eta} F(\eta; p) \right) - \tau Sc \left(\frac{\partial \Theta(\eta; p)}{\partial \eta} \frac{\partial \Phi(\eta; p)}{\partial \eta} + \Phi \frac{\partial^2 \Theta(\eta; p)}{\partial \eta^2} \right) \quad (29)$$

and R_f, R_θ , and R_ϕ are the non-zero auxiliary functions. In particular, $R_f = R_\theta = R_\phi = 1$.

3.2. *M*th-order deformation

To get the deformation equation of *m*th order, we have to differentiate *m* times the zeroth-order deformation equation (18) w.r.t. *p* at *p* = 0 and then have to divide the resulting expression by *m*!. Thus we have

$$L_f[f_m(\eta) - \chi_m f_{m-1}(\eta)] = h_f R_m^f(\eta), \quad (30)$$

$$L_\theta[\theta_m(\eta) - \chi_m \theta_{m-1}(\eta)] = h_\theta R_m^\theta(\eta), \quad (31)$$

$$L_\phi[\phi_m(\eta) - \chi_m \phi_{m-1}(\eta)] = h_\phi R_m^\phi(\eta) \quad (32)$$

with boundary conditions

$$f_m''(0) = 0, f_m(0) = 0, f_m(\infty) = 0, \quad (33)$$

$$\theta_m'(0) = \phi_m'(0) = 0, \theta_m'(\infty) = \phi_m'(0) = 0, \quad (34)$$

where

$$R_m^f = f_{m-1}''' - M f_{m-1}' \sin^2 \alpha + \sum_{k=0}^{m-1} f_{m-1-k} f_k'' - \sum_{k=0}^{m-1} f_{m-1-k}' f_k', \quad (35)$$

$$R_m^\theta = \theta_{m-1}'' + \text{Pr} \left[\sum_{k=0}^{m-1} f_k \theta_{m-1-k}' - 2 \sum_{k=0}^{m-1} \theta_k f_{m-1-k}' \right], \quad (36)$$

$$R_m^\phi = \phi_{m-1}'' + \text{Sc} \sum_{k=0}^{m-1} [f_k \phi_{m-1-k}' - 2 f_{m-1-k}' \phi_k] - \tau \text{Sc} \sum_{k=0}^{m-1} [\theta_k' \phi_{m-1-k}' + \theta_{m-1-k}'' \phi_k] \quad (37)$$

$$\text{with } \chi_m = \begin{cases} 1, & m > 1 \\ 0, & m \leq 1. \end{cases}$$

For *p* = 0 and for *p* = 1, we have

$$F(\eta; 0) = f_0(\eta), F(\eta; 1) = f(\eta) \quad (38)$$

$$\Theta(\eta; 0) = \theta_0(\eta), \Theta(\eta; 1) = \theta(\eta), \quad (39)$$

$$\Phi(\eta; 0) = \phi_0(\eta), \Phi(\eta; 1) = \phi(\eta) \quad (40)$$

and when *p* varies from 0 to 1, $F(\eta; p)$, $\Theta(\eta; p)$ and $\Phi(\eta; p)$ vary from the initial guesses $f_0(\eta)$, $\theta_0(\eta)$ and $\phi_0(\eta)$ to the final solutions $f(\eta)$, $\theta(\eta)$, and $\phi(\eta)$, respectively.

By means of Taylor's series, we have

$$\left. \begin{aligned} F(\eta; p) &= f_0(\eta) + \sum_{m=1}^{\infty} f_m(\eta) p^m, f_m(\eta) = \frac{1}{m!} \left(\frac{\partial^m F(\eta; p)}{\partial \eta^m} \right)_{p=0} \\ \Theta(\eta; p) &= \theta_0(\eta) + \sum_{m=1}^{\infty} \theta_m(\eta) p^m, \theta_m(\eta) = \frac{1}{m!} \left(\frac{\partial^m \Theta(\eta; p)}{\partial \eta^m} \right)_{p=0} \\ \Phi(\eta; p) &= \phi_0(\eta) + \sum_{m=1}^{\infty} \phi_m(\eta) p^m, \phi_m(\eta) = \frac{1}{m!} \left(\frac{\partial^m \Phi(\eta; p)}{\partial \eta^m} \right)_{p=0} \end{aligned} \right\} \quad (41)$$

Now, at $p = 1$,

$$\left. \begin{aligned} f(\eta) &= f_0(\eta) + \sum_{m=1}^{\infty} f_m(\eta), \\ \theta(\eta) &= \theta_0(\eta) + \sum_{m=1}^{\infty} \theta_m(\eta), \\ \phi(\eta) &= \phi_0(\eta) + \sum_{m=1}^{\infty} \phi_m(\eta), \end{aligned} \right\} \quad (42)$$

where

$$\left. \begin{aligned} f_m(\eta) &= f_m^*(\eta) + c_0 + c_1 e^\eta + c_2 e^{-\eta}, \\ \theta_m(\eta) &= \theta_m^*(\eta) + c_3 e^\eta + c_4 e^{-\eta}, \\ \phi_m(\eta) &= \phi_m^*(\eta) + c_5 e^\eta + c_6 e^{-\eta} \end{aligned} \right\} \quad (43)$$

are general solutions of Equations (30)–(32).

4. Convergence analysis

Liao [31] developed the average square residual errors as

$$\left. \begin{aligned} \varepsilon_m^f &= \frac{1}{k+1} \sum_{i=0}^k \left[N_f \left(\sum_{j=0}^m f(\eta) \right)_{\eta=i\delta\eta} \right]^2 \\ \varepsilon_m^\theta &= \frac{1}{k+1} \sum_{i=0}^k \left[N_\theta \left(\sum_{j=0}^m f(\eta), \sum_{j=0}^m \theta(\eta) \right)_{\eta=i\delta\eta} \right]^2 \\ \varepsilon_m^\phi &= \frac{1}{k+1} \sum_{i=0}^k \left[N_\phi \left(\sum_{j=0}^m f(\eta), \sum_{j=0}^m \theta(\eta), \sum_{j=0}^m \phi(\eta) \right)_{\eta=i\delta\eta} \right]^2 \end{aligned} \right\} \quad (44)$$

The total residual error ε_m^t is the sum of all individual residual errors, i.e. $\varepsilon_m^t = \varepsilon_m^f + \varepsilon_m^\theta + \varepsilon_m^\phi$.

In the present method, one of the key factors is the convergence rate of the solution. This convergence rate can be controlled by using different parameters in BVP 2.0. The values

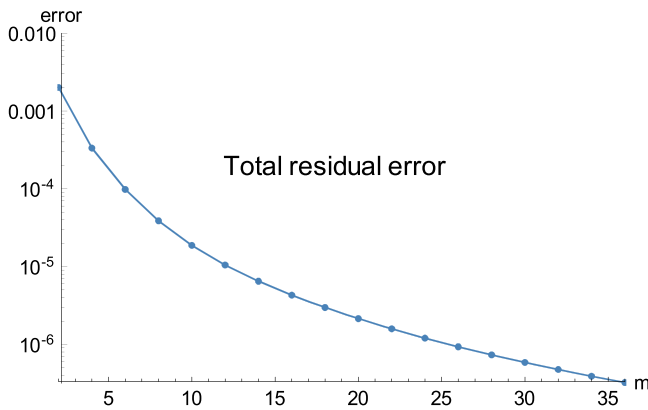


Figure 2. The total residual error.

Table 1. The choice of convergence control parameter when $M = 1.0$, $Pr = 0.71$, $Vc = -1.5$, $Sc = 0.22$, $Ma = 0.2$, $\tau = 0.5$, $\alpha = 45^\theta$.

k	h_f	h_θ	h_ϕ	Total error	CPU time
2	-0.307824	-0.654505	-1.34441	0.000467209	7.5629
4	-0.336042	-0.674788	-1.45105	0.000100105	41.4121
6	-0.356933	-0.702997	-1.51847	0.000039653	102.0410
8	-0.370781	-0.714897	-1.57082	0.000020084	259.8300

Table 2. The total estimated residual error when $M = 1.0$, $Pr = 0.71$, $Vc = -1.5$, $Sc = 0.22$, $Ma = 0.2$, $\tau = 0.5$, $\alpha = 45^\theta$ gained at $k = 8$.

k	ε_k^f	ε_k^θ	ε_k^ϕ
2	0.000266103	0.000269534	0.000361419
6	1.19419×10^{-6}	6.48936×10^{-6}	0.0000340312
14	4.43612×10^{-10}	4.36748×10^{-7}	4.97827×10^{-6}
22	4.36111×10^{-13}	8.29876×10^{-8}	1.62157×10^{-6}
30	6.28147×10^{-16}	2.18746×10^{-8}	6.85102×10^{-7}

of those parameters can be obtained by minimizing the error in BVPPh 2.0. In Table 1, we have presented the convergence control parameters for different iterations. From Table 1, it is clear that the choice of convergence control parameters is in decreasing manner, and hence, we calculate the estimated residual errors shown in Table 2 assuming control parameters as achieved at the eighth iteration level of Table 1. Figure 2 shows the combined total estimated residual error for 30th order of approximation in OHAM technique. To show the convergence of solutions of converted governing equations, the values of $f'(0)$, $-\theta'(0)$, and $-\phi'(0)$ are obtained for different orders of approximation. These convergent results by OHAM up to 30th-order approximation for convergence analysis of $f'(0)$, $-\theta'(0)$, and $-\phi'(0)$ are described in Table 3. Farooq et al. [52] gave detailed explanations about the Mathematica package BVPPh 2.0 and optimal convergence control parameters. Some other important contributions where OHAM is used via BVPPh 2.0 may be found in the literature [53–55].

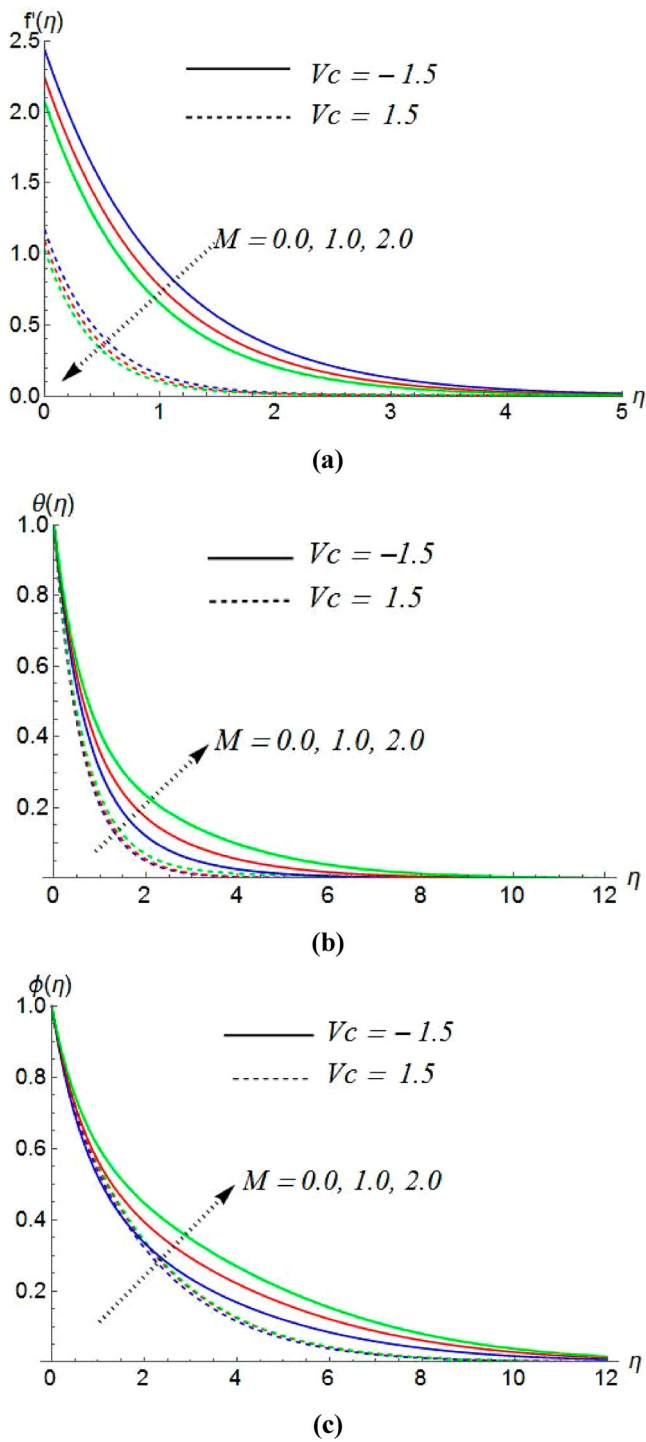


Figure 3. Impacts of M on (a) velocity, (b) temperature, and (c) concentration with suction and injection.

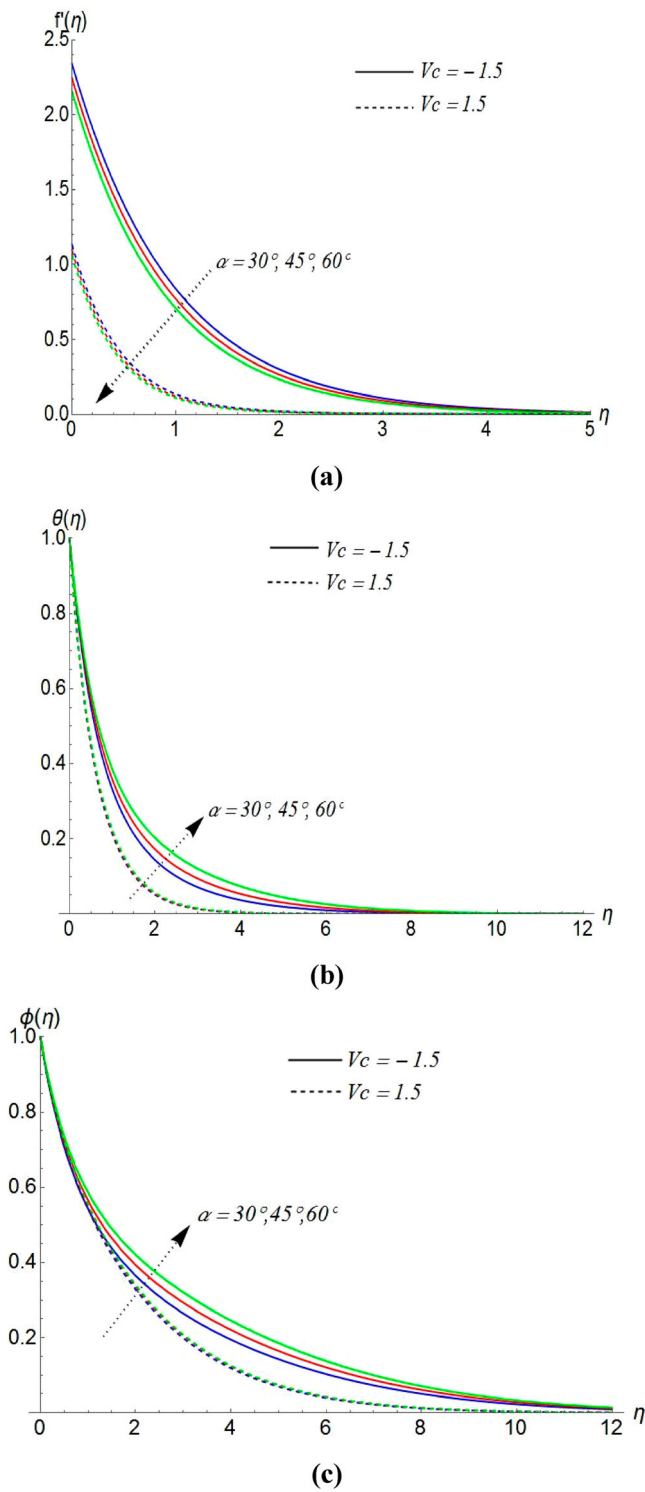


Figure 4. Impacts of α on (a) velocity, (b) temperature, and (c) concentration with suction and injection.

5. Results and discussion

Semi-analytical OHAM solutions for velocity, temperature, and concentration and their variations with thermophoretic velocity, aligned magnetic field, Marangoni convection are obtained and presented in some figures and tables. For the calculation purpose, we have chosen some fixed values of involved parameters when those are not in varying state and those are $M = 1$, $Ma = 0.2$, $Pr = 0.71$, $Sc = 0.22$, $\tau = 0.5$, $\alpha = 0.45^\circ$, $Vc = 1.5$ and -1.5 . While the parameters are considered as variables to demonstrate the consequences of above-mentioned heat transfer, mass transfer, and flow properties for MHD boundary layer.

For validity as well as the correctness of the used semi-analytical approach, we have compared our calculated values of $f'(0)$ with the data provided by Mahdy and Ahmed [16] obtained using the fourth-order RK method, Zhang and Zheng [14] obtained using the perturbation expansion method (with Pade approximation) and Das et al. [47] obtained using MATLAB inbuilt 'bvp4c' technique for various value of magnetic parameter in Table 4. In the comparison table, it may be witnessed that those sets of results are nicely agreed with the results of the present investigation and consequently, it may be confidently concluded that the obtained OHAM solutions are pretty correct.

Figure 3 explores the influences of the magnetic field on velocity distribution, temperature, and concentration, while both suction and injection are considered separately. For a stronger magnetic field velocity reduces, whereas temperature and concentration rise. Physically, the existence of a magnetic field produces a resisting type force called 'Lorentz force'. The nature of the Lorentz force is to reduce the movement of fluid and also it is responsible for enhancements in temperature as well as concentration distribution. But, it is interestingly notable that in presence of injection the influences of magnetic parameter M are more prominent. Whereas the changes in velocity, temperature, and concentration for variation in the inclination angle of the aligned magnetic field are exhibited in Figure 4 with imposed suction and injection in the flow field. It shows that in both cases, for the growth of inclination angle velocity decreases, while temperature and concentration are

Table 3. Convergence table for $f'(0)$, $-\theta'(0)$, and $-\phi'(0)$ for the different order of approximations.

Order of approximation	$f'(0)$	$-\theta'(0)$	$-\phi'(0)$
2	2.2585	1.2021	0.8144
8	2.2458	1.2171	0.7783
18	2.2455	1.2168	0.7488
24	2.2455	1.2166	0.7467
26	2.2455	1.2166	0.7462
28	2.2455	1.2166	0.7457
30	2.2455	1.2166	0.7457

Table 4. Comparison of $f'(0)$ with previously published result for $\alpha = 90^\circ$ ($\sin \alpha = 1$), $\tau = 0$, $Pr = 0.78$, $Sc = 0.6$, $Vc = 0$, $Ma = 1$.

M	$f'(0)$			
	Zhang and Zheng [14]	Das et al.[37]	Mahdy and Ahmed [16]	Present study
0	2.4569	2.45557	2.519945	2.5199881
1	2.1572	2.15688	2.226772	2.2267723
4	1.6240	1.62511	1.6785735	1.6786231

showing increasing status and in the case of mass injection the impacts of inclination angle are intensified. It means that if the magnetic field is orthogonal to the flat surface then the Lorentz force has its maximum impact.

Figure 5 illustrated the nature of the boundary layer flow properties with positive submission of thermosolutal ratio Ma . The figure discloses that an increment in Ma the velocity near surface significantly enhances and opposite nature is observed away from the plate for mass injection case. Physically, by growing the Marangoni convection parameter, additional induced flow occurs and it initiates at the surface. For mass injection, the spread of induced flow is unable to occur in the whole boundary layer, i.e. it causes the acute velocity gained near the wall, but velocity away from the plate shows a decreasing nature. For the mass suction case, the aforesaid impact of Marangoni convection on velocity has been witnessed in the whole boundary layer region. Whereas thermosolutal Marangoni convection causes diminutions of temperature and concentration inside the boundary layer.

Now, to know the impressions of suction/injection parameter on velocity, temperature, and concentration separately, computed data are presented in Figure 6. The existence mass suction through tiny pores in the heated flat surface originates reductions of velocity, temperature, and concentration, whereas mass injection causes reverse impacts. As a result of raising suction ($V_c > 0$) fluid layers away from the plate come closer, which is the reason for declines in velocity, temperature, and concentration with suction and contrastingly, these observations are found to be in a reverse manner in the positive exposition of injection ($V_c < 0$). Figure 7 shows that the positive submission in the value of Pr number reduces the temperature, whereas the incremental value of Sc produces diminution in the concentration. With increments of Pr and Sc , there exist respective growths of thermal conductivity and mass diffusivity and consequently, the decays of thermal and concentration boundary layer thicknesses along with temperature and concentration are witnessed. For both suction and injection, concentration reduces with the thermophoretic effect. These declines in concentration are similar for suction and injection and it confirms the independency of thermophoresis on suction/injection for the case of thermosolutal Marangoni convection. Physically, when thermophoresis occurs the suspended solute particles are attracted away from a hot flat plate towards a cooler place and which results this reduction.

For several values of magnetic and suction/injection parameters and Marangoni number, variations in $f'(0)$, $-\theta'(0)$ and $-\phi'(0)$ which are directly related to surface velocity, Nusselt and Sherwood numbers are explained in Figure 8. It is noticed that in the presence of suction/injection, wall velocity declines with magnetic parameter (due to Lorentz force) and it increases for Marangoni number (for induced velocity near the plate). Whereas, Nusselt and Sherwood numbers show improving character with increasing Marangoni number, but Nusselt number reduces with raising value of magnetic parameter for both suction and injection. For a smaller value of magnetic parameter, Sherwood number displays reducing nature with suction/injection parameter and for a higher value of M , it exhibits contradictory character, i.e. higher Lorentz force completely changes the influence of suction/injection. The above facts may be re-verified from Tables 5 and 6.

6. Conclusion

Thermosolutal Marangoni convection on a permeable flat surface with an aligned magnetic field and thermophoretic velocity is investigated. In the whole analysis, influences of

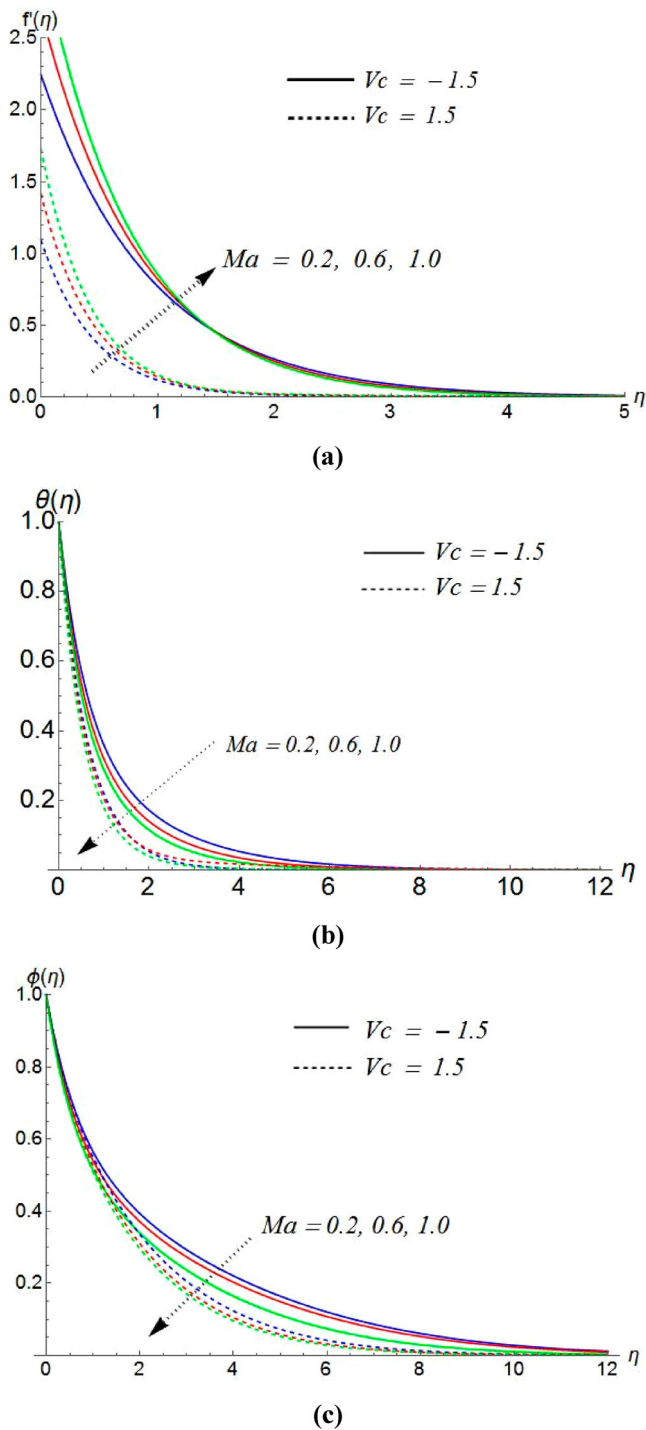


Figure 5. Impacts of Ma on (a) velocity, (b) temperature, and (c) concentration with suction and injection.

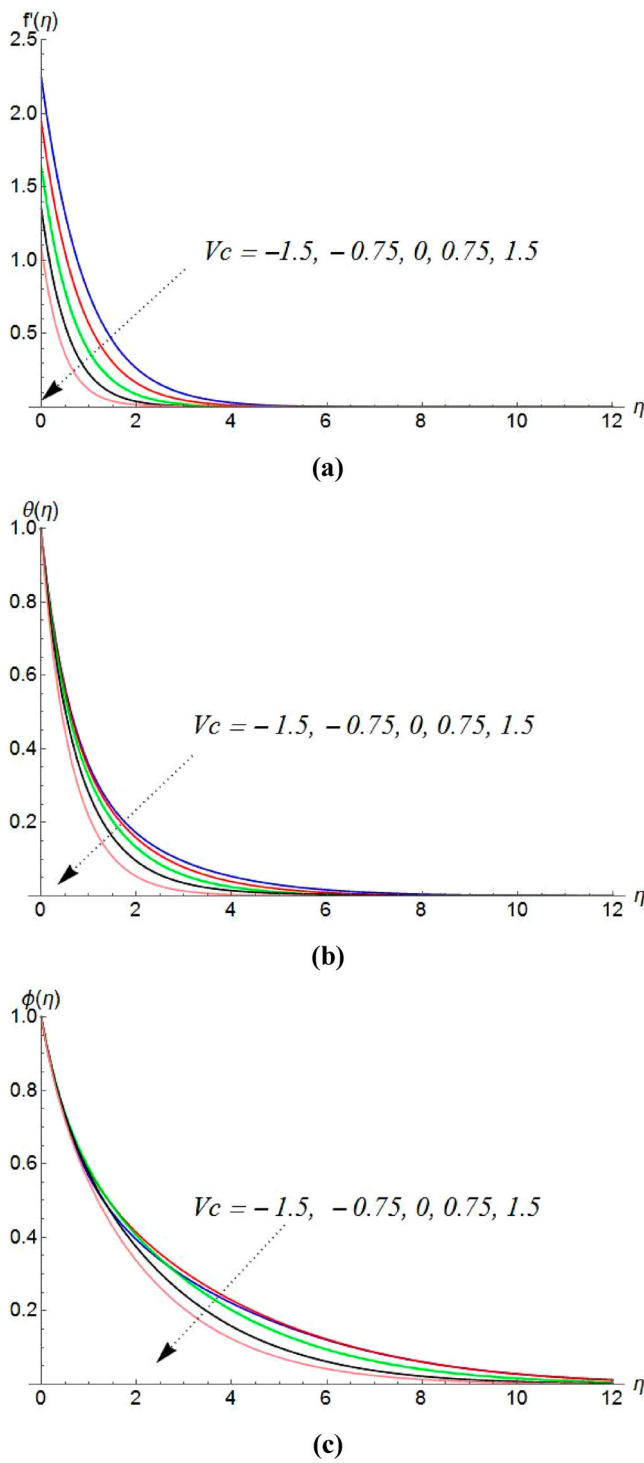


Figure 6. Impacts of Vc on (a) velocity, (b) temperature, and (c) concentration.

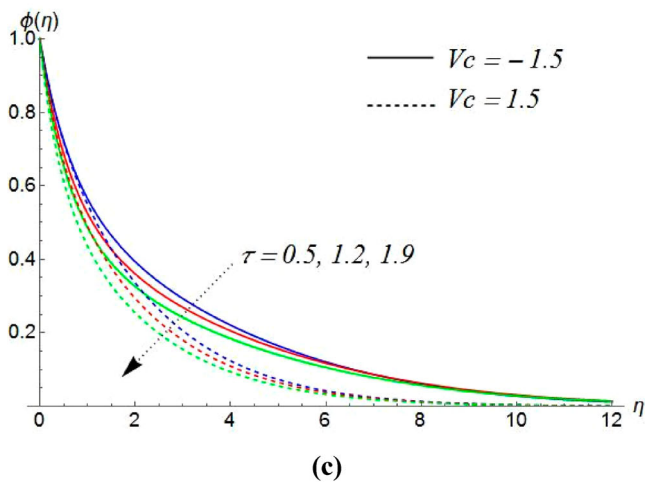
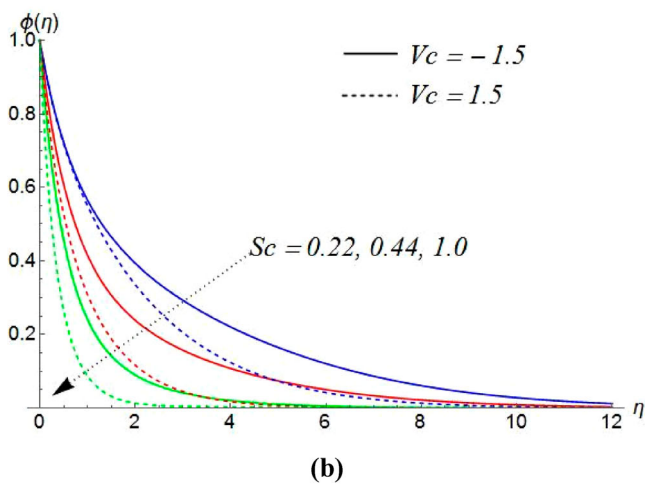
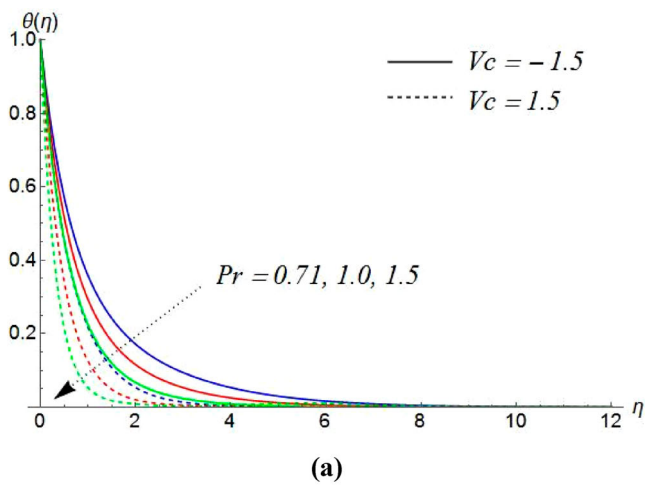
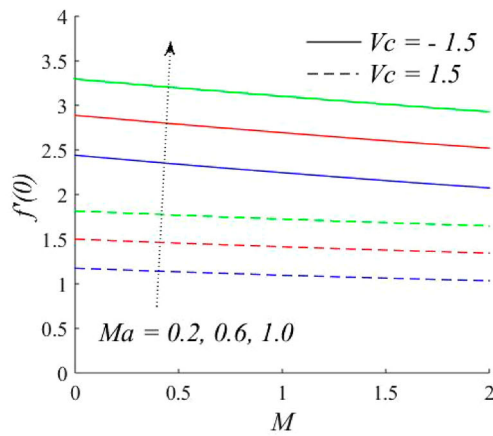
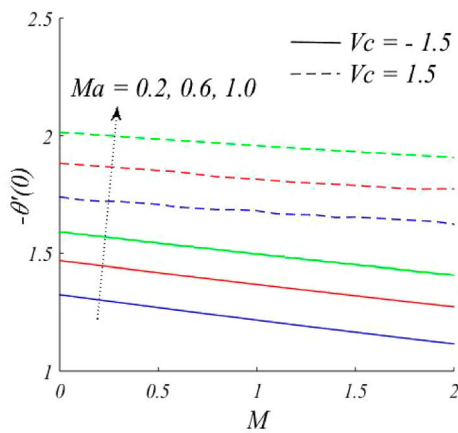


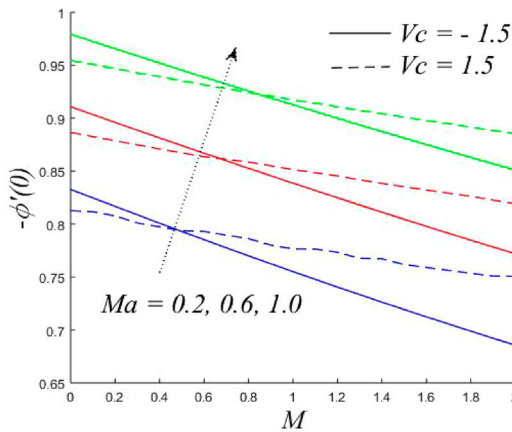
Figure 7. Impacts of (a) Pr on temperature, (b) Sc on concentration, and (c) τ on concentration with suction and injection.



(a)



(b)



(c)

Figure 8. Impacts of Ma and M on (a) surface velocity, (b) Nusselt number, and (c) Sherwood number with suction and injection.

Table 5. Variation in $f'(0)$ and $-\theta'(0)$ for different parameters.

M	Values of different parameters		$f'(0)$		$-\theta'(0)$	
	Ma	α	$Vc = -1.5$	$Vc = 1.5$	$Vc = 1.5$	$Vc = 1.5$
0	0.2	45^θ	2.4412599	1.17437066	1.324900	1.7394153
1			2.2456259	1.09441018	1.217174	1.6805585
2			2.0743615	1.03313325	1.116141	1.6236013
1	0.2		2.2456259	1.09441018	1.217174	1.6805585
	0.6		2.6937485	1.41502573	1.368711	1.8150276
	1		3.1020812	1.72532463	1.496992	1.9575860
	0.2	30^θ	2.3402494	1.13337724	1.270441	1.7082173
		45^θ	2.2456259	1.09441018	1.217174	1.6805585
		60^θ	2.1570983	1.06321794	1.165687	1.6543074

Table 6. Calculated values of $-\phi'(0)$ for different parameters.

Values of different parameters			$-\phi'(0)$		
M	Ma	α	τ	$Vc = -1.5$	$Vc = 1.5$
0	0.2	45^θ		0.8326645	0.8126390
1				0.7550794	0.7766225
2				0.6855907	0.7505730
1	0.2			0.7550794	0.7766225
	0.6			0.8386411	0.8515201
	1			0.9126470	0.9173194
	0.2	30^θ		0.7929431	0.7937333
		45^θ		0.7550794	0.7766225
		60^θ		0.7192704	0.7617858
		45^θ	0.5	0.7550794	0.7766225
			1.2	0.8939349	1.0197334
			1.9	1.0349270	1.2658398

suction and injection both are considered simultaneously. The nonlinear system of PDEs is executed by a suitable transformation and after that, the semi-analytical OHAM solutions have been obtained from converted ODEs. The major findings of the study have been listed below:

- In both cases, i.e. for suction and injection, larger values of the magnetic parameter and inclination angle produce a reduction effect on velocity, while opposite impacts on temperature and concentration are noticed. Interestingly, these impacts display dominance for injection in the flow field.
- For an orthogonal magnetic field to the flat surface, the generated Lorentz force shows maximum resistance for the transport phenomenon.
- In presence of injection, with the rising value of Marangoni parameter, there is an enhancement in velocity near the plate, while for suction velocity enhancement is witnessed in the entire boundary layer region. Whereas, decreasing characters are found in temperature and concentration for Marangoni convection.
- Mass suction(injection) originates reductions(rises) in temperature, velocity, and concentration.
- Larger Prandtl number produces smaller thermal boundary layer thickness, similar impact on concentration is witnessed for higher Schmidt number.
- For growth in thermophoretic velocity, concentration is driven towards a decrement.

- For increment in magnetic parameter, wall velocity declines and it rises with Marangoni number. Similar trends are experienced in Nusselt number, i.e. heat transfer rate.
- For small magnetic parameter, mass transfer rate drops with suction/injection parameter, whereas for higher magnetic parameter it augments.

Acknowledgements

The authors are grateful to the reviewers for their precious comments and suggestions. K. Bhattacharyya acknowledges 'Faculty Incentive Grant' (No. R/Dev/D/loE/Incentive/2022-23/47686) of Banaras Hindu University.

Disclosure statement

No potential conflict of interest was reported by the author(s).

Funding

This work was supported by Banaras Hindu University: [Grant Number R/Dev/D/loE/Incentive/2022-23/47686].

ORCID

Krishnendu Bhattacharyya  <http://orcid.org/0000-0001-7975-0709>

Dhananjay Yadav  <http://orcid.org/0000-0001-8404-2053>

References

- [1] Tsou FK, Sparrow EM, Goldstein RJ. Flow and heat transfer in the boundary layer on a continuous moving surface. *Int J Heat Mass Transfer*. 1967;10(2):219–235.
- [2] Aydin O, Kaya A. Laminar boundary layer flow over a horizontal permeable flat plate. *Appl Math Comput*. 2005;161(1):229–240.
- [3] Hussain S, Hossain MA, Wilson M. Natural convection flow from a vertical permeable flat with variable surface temperature and species concentration. *Eng Comput*. 2000;17(7):789–812.
- [4] Aziz A. A similarity solution for laminar thermal boundary layer over a flat plate with a convective surface boundary condition. *Commun Nonlinear Sci Numer Simul*. 2009;14(4):1064–1068.
- [5] Glauert MB. A study of magnetohydrodynamic boundary layer flow on a flat plate. *J Fluid Mech*. 1961;10(2):276–288.
- [6] Pop I, Na TY. A note on MHD flow over a permeable stretching surface. *Mech Res Commun*. 1998;25(3):263–269.
- [7] Levich VG. *Physicochemical hydrodynamics*. Prentice-Hall; 1962; 163.
- [8] Magyari E, Chamka AJ. Exact analytical solutions for thermosolutal marangoni convection in the presence of heat and mass generation or consumption. *Heat Mass Transfer*. 2007;43:965–974.
- [9] Magyari E, Chamka AJ. Exact analytical result for the thermosolutal MHD marangoni boundary layer. *Int J Therm Sci*. 2008;47:848–857.
- [10] Pascal JP, D'Alessio SJD. Thermosolutal marangoni effect on the inclined flow of a binary liquid with variable density. I. linear stability analysis. *Physical Review Fluids*. 2016;1(8):083603.
- [11] Napolitano LG, Golia C. Coupled marangoni boundary layers. *Acta Astronaut*. 1981;8(5-6):417–434.
- [12] Chamka AJ, Pop I, Thakar HS. Marangoni mixed convection boundary layer flow. *Meccanica*. 2006;41:219–232.
- [13] Tadmor R. Marangoni flow revisited. *J Colloid Interface Sci*. 2009;332:451–454.

- [14] Zhang Y, Zheng L. Analysis of MHD thermosolutal Marangoni convection with the heat generation and a first order chemical reaction. *Chem Eng Sci.* 2012;69(1):449–455.
- [15] Al-Mudhaf A, Chamka AJ. Similarity solutions for MHD thermosolutal Marangoni convection over a flat surface in the presence of heat generation or absorption effects. *Heat Mass Transfer.* 2005;42(2):112–121.
- [16] Mahdy A, Ahmed SE. Thermosolutal Marangoni boundary layer magnetohydrodynamics flow with the Soret and Dufour effects past a vertical flat plate. *Eng Sci Technol An Int J.* 2015;18(1):24–31.
- [17] Mahabaleshwar US, Nagaraju KR, Kumar PNV, et al. Effect of radiation on thermosolutal Marangoni convection in a porous medium with chemical reaction and heat source/sink. *AIP Adv.* 2020;32.
- [18] Al-Mdallal QM, Indumathi M, Ganga B, et al. Marangoni radiative effect of hybrid nanofluids flow past a permeable surface with inclined magnetic field. *Case Stud Therm Eng.* 2020;17:100571.
- [19] Hakeem AKA, Indumathi N, Ganga B, et al. Comparison of disparate solid volume fraction ratio of hybrid nanofluids flow over a permeable flat surface with aligned magnetic field and Marangoni convection. *Scientia Iranica Trans F Nanotechnol.* 2020;27(6):3367–3380.
- [20] Hatami M, Ganji DD. Motion of a spherical particle in a fluid forced vortex by DQM and DTM. *Particuology.* 2014;16:206–212.
- [21] Pourmehran O, Rahimi-Gorji M, Hatami M, et al. Numerical optimization of microchannel heat sink (MCHS) performance cooled by KKL based nanofluids in saturated porous medium. *J Taiwan Inst Chem Eng.* 2015;55:49–68.
- [22] Song D, Hatami M, Wang Y, et al. Prediction of hydrodynamic and optical properties of TiO₂/water suspension considering particle size distribution. *Int J Heat Mass Transfer.* 2016;92:864–876.
- [23] Hatami M, Safari H. Effect of inside heated cylinder on the natural convection heat transfer of nanofluids in a wavy-wall enclosure. *Int J Heat Mass Transfer.* 2016;103:1053–1057.
- [24] Ghasemi SE, Vatani M, Hatami M, et al. Analytical and numerical investigation of nanoparticle effect on peristaltic fluid flow in drug delivery systems. *J Mol Liq.* 2016;215:88–97.
- [25] Hatami M, Song D, Jing D. Optimization of a circular-wavy cavity filled by nanofluid under the natural convection heat transfer condition. *Int J Heat Mass Transfer.* 2016;98:758–767.
- [26] Hatami M. Nanoparticles migration around the heated cylinder during the RSM optimization of a wavy-wall enclosure. *Adv Powder Technol.* 2017;28:890–899.
- [27] Hatami M. Numerical study of nanofluids natural convection in a rectangular cavity including heated fins. *J Mol Liq.* 2017;233:1–8.
- [28] Mosayebidorcheh S, Hatami M. Analytical investigation of peristaltic nanofluid flow and heat transfer in an asymmetric wavy wall channel (Part I: straight channel). *Int J Heat Mass Transfer.* 2018;126:790–799.
- [29] Reddy SRR, Reddy PBA, Bhattacharyya K. Effect of nonlinear thermal radiation on 3D magneto slip flow of Eyring–Powell nanofluid flow over a slendering sheet inspired through binary chemical reaction and Arrhenius activation energy. *Adv Powder Technol.* 2019;30(12):3203–3213.
- [30] Verma AK, Gautam AK, Bhattacharyya K, et al. Entropy generation analysis in Falkner–Skan flow of Maxwell nanofluid in Darcian porous medium with temperature-dependent variable viscosity. *Pramana – Journal of Physics.* 2021;95(2):69.
- [31] Verma AK, Gautam AK, Bhattacharyya K, et al. Boundary layer flow of non-Newtonian Eyring–Powell nanofluid over a moving flat plate in Darcy porous medium with a parallel free-stream: multiple solutions and stability analysis. *Pramana J Phys.* 2021;95(4):173.
- [32] Banerjee A, Bhattacharyya K, Mahato SK, et al. Influence of various shapes of nanoparticles on unsteady stagnation-point flow of Cu-H₂O nanofluid on a flat surface in porous medium: a stability analysis. *Chin Phys B.* 2022;31(04):044701.
- [33] Verma AK, Rajput S, Bhattacharyya K, et al. Nanoparticle's radius effect on unsteady mixed convective copper-water nanofluid flow over an expanding sheet in porous medium with boundary slip. *Chem Eng J Adv.* 2022;12:100366.
- [34] Rajput S, Verma AK, Bhattacharyya K, et al. Unsteady nonlinear mixed convective flow of nanofluid over a wedge: Buongiorno model. *Waves Random Complex Media.* 2021. doi:10.1080/17455030.2021.1987586

- [35] Rajput S, Bhattacharyya K, Verma AK, et al. Unsteady stagnation-point flow of CNTs suspended nanofluid on a shrinking/expanding sheet with partial slip: multiple solutions and stability analysis. *Waves Random Complex Media*. 2022. doi:10.1080/17455030.2022.2063986
- [36] Talbot L, Cheng RK, Schefer RW, et al. Thermophoresis of a particle in a heated boundary layer. *J Fluid Mech*. 1980;101(4):737–758.
- [37] Uddin MJ, Ali MY. Effects of hydromagnetic and thermophoresis of unsteady forced convection boundary layer flow over flat plates. *J Appl Math Phys*. 2016;4(9):1756–1776.
- [38] Bakier AY, Gorla R. Effects of thermophoresis and radiation on laminar flow along a semi-infinite vertical plate. *Heat Mass Transfer*. 2011;47(4):419–425.
- [39] Postelnicu A. Thermophoresis particle deposition in natural convection over inclined surface in porous media. *Int J Heat Mass Transfer*. 2012;55(7–8):2087–2094.
- [40] Kundu PK, Das K, Jana S. Impact of chemical reaction on MHD mixed convection heat and mass transfer flow with thermophoresis. *Walailak J Sci Technol*. 2013;11(2):149–170.
- [41] Parida SK, Panda S, Rout BR. MHD boundary layer slip flow and radiative nonlinear heat transfer over a flat plate with variable fluid properties and thermophoresis. *Alexandria Eng J*. 2015;54(4):941–953.
- [42] Salim A, Hossain MA, Rees DAS. The effect of surface mass transfer on mixed convection flow past a heated vertical flat permeable flat plate with thermophoresis. *Int J Therm Sci*. 2003;42(10):973–982.
- [43] Chamkha AJ, Issa C. Effect of heat generation and absorption on thermophoresis on hydromagnetic flow with heat and mass transfer over a flat surface. *Int J Numer Methods Heat Fluid Flow*. 2000;10(4):432–448.
- [44] Alam MS, Rahman MM, Sattar MA. Effects of variable suction and thermophoresis on steady MHD combined free-forced convective heat and mass transfer flow over a semi-infinite permeable inclined plate in the presence of thermal radiation. *Int J Therm Sci*. 2008;47(6):758–765.
- [45] Alam MS, Rahman MM, Sattar MA. Effects of chemical reaction, thermophoresis and heat generation/absorption on steady MHD mixed convective heat and mass transfer flow along a semi-infinite inclined porous flat plate with viscous dissipation and joule heating. *Can J Phys*. 2008;86:1057–1066.
- [46] Alam MS, Rahman MM, Sattar MA. On the effectiveness of viscous dissipation and joule heating on steady magnetohydrodynamic heat and mass transfer flow over an inclined radiate isothermal permeable surface in the presence of thermophoresis. *Commun Nonlinear Sci Numer Simul*. 2009;14(5):2132–2143.
- [47] Das K, Acharya N, Kundu PK. Effect of magnetic field on thermosolutal Marangoni boundary layer flow. *Acta Technica*. 2015;60:237–252.
- [48] Hamid RA, Zaimi WMKAW, Arifin NM, et al. Thermal diffusion and diffusion thermo effects on MHD thermosolutal Marangoni convection boundary layer flow over a permeable surface. *J Appl Math*. 2012;2012:750939.
- [49] Hayat T, Khan MI, Farooq M, et al. Impact of Marangoni convection in the flow of carbon–water nanofluid with thermal radiation. *Int J Heat Mass Transfer*. 2017;106:810–815.
- [50] Pal D, Chatterjee S. Mixed convection magnetohydrodynamic heat and mass transfer past a stretching surface in a micropolar fluid-saturated porous medium under the influence of Ohmic heating, Soret and Dufour effects. *Commun Nonlinear Sci Numer Simul*. 2011;16:1329–1346.
- [51] Liao S. Homotopy analysis method in nonlinear differential equations. Springer; 2012.
- [52] Farooq U, Zhao YL, Hayat T, et al. Application of HAM based Mathematica package BVPh 2.0 on MHD Falkner-Skan. *Comput Fluid*. 2015;111:69–75.
- [53] Jafeer MB, Mustafa M. A study of elastic-viscous fluid flow by revolving disk with heat dissipation effects using HAM package BVPh 2.0. *Sci Rep*. 2021;11:4514.
- [54] Hayat T, Khan SA, Alsaedi A. Simulation and modeling of entropy optimized MHD flow of second grade fluid with dissipation effect. *J Mater Res*. 2020;9(5):11993–12006.
- [55] Muhammad K, Hayat T, Alsaedi A. OHAM analysis of fourth-grade nonmaterial in the presence of stagnation point and convective heat-mass conditions. *Wave Random Complex Media*. 2021. doi:10.1080/17455030.2021.1892865.